APL Materials

Engineering the magnetic order in epitaxially strained $Sr_{1-x}Ba_xMnO_3$ perovskite thin films

Cite as: APL Mater. **7**, 041117 (2019); https://doi.org/10.1063/1.5090824
Submitted: 30 January 2019 . Accepted: 14 April 2019 . Published Online: 24 April 2019

L. Maurel, N. Marcano, E. Langenberg, R. Guzmán, T. Prokscha, C. Magén, J. A. Pardo, and P. A. Algarabel

APL Materials ARTICLE scitation.org/journal/apm

Engineering the magnetic order in epitaxially strained $Sr_{1-x}Ba_xMnO_3$ perovskite thin films

Cite as: APL Mater. 7, 041117 (2019); doi: 10.1063/1.5090824
Submitted: 30 January 2019 • Accepted: 14 April 2019 •
Published Online: 24 April 2019

L. Maurel,[1,2,a)] N. Marcano,[3,4,b)] E. Langenberg,[1,4] R. Guzmán,[5] T. Prokscha,[6] C. Magén,[1,4,5] J. A. Pardo,[2,4,5,7] and P. A. Algarabel[1,4]

AFFILIATIONS

[1]Departamento de Física de la Materia Condensada, Universidad de Zaragoza, 50009 Zaragoza, Spain
[2]Instituto de Nanociencia de Aragón (INA), Universidad de Zaragoza, 50018 Zaragoza, Spain
[3]Centro Universitario de la Defensa, Academia General Militar, 50090 Zaragoza, Spain
[4]Instituto de Ciencia de Materiales de Aragón (ICMA), Universidad de Zaragoza-CSIC, 50009 Zaragoza, Spain
[5]Laboratorio de Microscopías Avanzadas, Universidad de Zaragoza, 50018 Zaragoza, Spain
[6]Laboratory for Muon Spin Spectroscopy, Paul Scherrer Institut, CH-5232 Villigen PSI, Switzerland
[7]Departamento de Ciencia y Tecnología de Materiales y Fluidos, Universidad de Zaragoza, 50018 Zaragoza, Spain

[a)]**Current address:** Laboratory for Mesoscopic Systems, Department of Materials, ETH Zurich, 8093 Zurich, Switzerland and Laboratory for Multiscale Materials Experiments, Paul Scherrer Institut, 5232 Villigen PSI, Switzerland
[b)]**Author to whom correspondence should be addressed:** marcanon@unizar.es

ABSTRACT

Chemical doping and epitaxy can be used to tailor the magnetoelectric properties of multiferroic thin films, such as $SrMnO_3$. Here, we study the dependence of the magnetic order temperatures of $Sr_{1-x}Ba_xMnO_3$ thin films on epitaxial strain and Ba content. Combining low-energy muon spin spectroscopy and scanning transmission electron microscopy, the broadness of the magnetic transition is attributed to the presence of a Mn-O-Mn angle gradient along the out-of-plane direction. We also demonstrate that the unit cell volume is the key parameter to determine the Néel temperature in $Sr_{1-x}Ba_xMnO_3$ thin films showing G-type antiferromagnetic order. The occurrence of a simultaneously ferroelectric and ferromagnetic ground state at high strain levels is suggested for the $Sr_{0.8}Ba_{0.2}MnO_3$ thin film deposited on $TbScO_3$.

Research on multiferroics (materials showing two or more ferroic orders) has been mainly focused on the design and study of magnetoelectric materials with an effective coupling between these orders that would allow commuting the conjugate fields and so controlling the magnetic response by applying an electric field and vice versa. A strong magnetoelectric coupling at room temperature is a basic requirement for introducing these materials into novel devices with potential applications in the field of spintronics, data storage, and sensors.[1–3]

$Sr_{1-x}Ba_xMnO_3$ (SBMO) perovskites stand out as promising multiferroic materials due to the strong coupling between polar instability, spin order, and lattice expected in these compounds. The expansion of the lattice by either epitaxial strain engineering or chemical pressure (replacing Sr with Ba) favors noncentrosymmetric distortions.[4–9] This was experimentally confirmed by turning bulk centrosymmetric $SrMnO_3$ (SMO) into polar in strained (strain ≥ 1.7%) epitaxial thin films,[10,11] and by inducing ferroelectricity in bulk SBMO for $x > 0.4$.[12,13] The coupling between lattice and spin enables a moderate epitaxial strain to modify the magnetic interactions and eventually the magnetic ground states in SMO.[6,8,9,11,14] Indeed, a crossover from G-type to C-type antiferromagnetic order was proposed by different groups at a critical tensile strain of 1.6%[6] or ≈3%.[9] The magnetic order strongly couples with the polar instability since both are driven by the Mn cation,[5–7,12,13,15] thus giving rise to a strong magnetoelectric coupling.[16,17]

According to the observations previously reported, epitaxial films of SBMO perovskite are ideal candidates for tailoring the magnetoelectric coupling by modifying the magnetic and electrical

properties through the accurate control of Ba content and epitaxial strain. The perovskite phase in epitaxial SBMO films was synthesized for the first time by Langenberg *et al.* with Ba contents in the range of $0.2 \leq x \leq 0.5$ on different perovskite substrates.[18] The combination of epitaxial strain and chemical pressure yields severe structural changes in SBMO in which much larger tetragonal distortions can be imposed than in bulk specimens.[18] Magnetoelectric coupling in bulk SBMO was indirectly observed by Sakai *et al.* by measuring the decrease in the tetragonality on the onset of the paramagnetic (PM) to antiferromagnetic (AF) transition.[12] For strained SMO thin films, a decrease in the emitted second harmonic signal, proportional to the square of the electric polarization, was also observed at the PM-AF transition.[10] Recently, our group has demonstrated the existence of a strong spin-phonon coupling at the Néel temperature (T_N) in epitaxial $Sr_{0.6}Ba_{0.4}MnO_3$ thin films.[19] Moreover, we have found that the dielectric constant drops by up to 50% when the AF order emerges and, more important, this coupling between magnetism and dielectric properties can be tuned from ≈18% to ≈50% by appropriately selecting both Ba-content and epitaxial strain.[20]

To date, most studies on the dependence of the magnetic order temperature (T_{order}) with the Ba content of SBMO have been done in bulk samples,[12,13,21] obtaining a decrease in T_N with increasing x. Regarding the impact of strain, Maurel *et al.* reported the decrease in T_N with the epitaxial strain in SMO thin films.[14] Recent *ab initio* calculations predicted that $Sr_{0.5}Ba_{0.5}MnO_3$ becomes ferromagnetic above a critical value of tensile epitaxial strain[8] and simultaneously ferromagnetic and ferroelectric at large enough compressive strain.[22] In this letter, we report on a comprehensive investigation of the magnetic order of SBMO perovskite epitaxial thin films by combining the Ba content and epitaxial strain. For this purpose, we have selected films with Ba compositions x = 0, 0.2, 0.4, and 0.5 grown on two different substrates: $(LaAlO_3)_{0.3}$-$(Sr_2AlTaO_6)_{0.7}$ (LSAT) and $TbScO_3$ (TSO). For a given substrate, Ba doping induces changes in both the cell volume and strain, which allows studying the dependence of T_{order} on both parameters.

Films of single-phase SBMO perovskite were grown by pulsed laser deposition (PLD) onto (001)-oriented single-crystal substrates of LSAT and TSO, which have pseudocubic lattice parameters $a \approx 0.387$ nm and $a \approx 0.396$ nm, respectively. The growth, perovskite phase stability, and structure were reported elsewhere.[18] The thickness of the films was limited to 10 nm, assuring that all of them were fully strained. The structure, crystal quality, and epitaxial coherence of the films were evaluated using x-ray diffraction (XRD) and scanning transmission electron microscopy (HAADF-STEM).

Symmetric θ/2θ XRD scans measured with monochromatic Cu-$K\alpha_1$ radiation around the pseudocubic 002 reflection allowed us to obtain the out-of-plane (c) lattice parameter of the films; see Figs. 1(a) and 1(b). The resulting structural parameters are listed in Table I. Figures 1(c) and 1(d) display the dependence of the cell volume (V) and the tetragonality (c/a) on the Ba-content (x) for the films grown on LSAT and TSO, respectively. For the films grown on LSAT, a change in the tetragonality from $c/a < 1$ (tensile strain, for x = 0 and x = 0.2) to $c/a > 1$ (compressive strain, for x = 0.4) is induced by increasing the Ba content. For the films deposited on TSO, c/a increases by increasing the Ba doping but remains always below 1 (tensile strain). As expected, the progressive replacement of Sr^{2+} cations (with ionic radius r = 1.44 Å in octahedral coordination[23]) with the larger Ba^{2+} cations (r = 1.60 Å) produces a gradual expansion of the unit cell volume for the films deposited on both substrates.

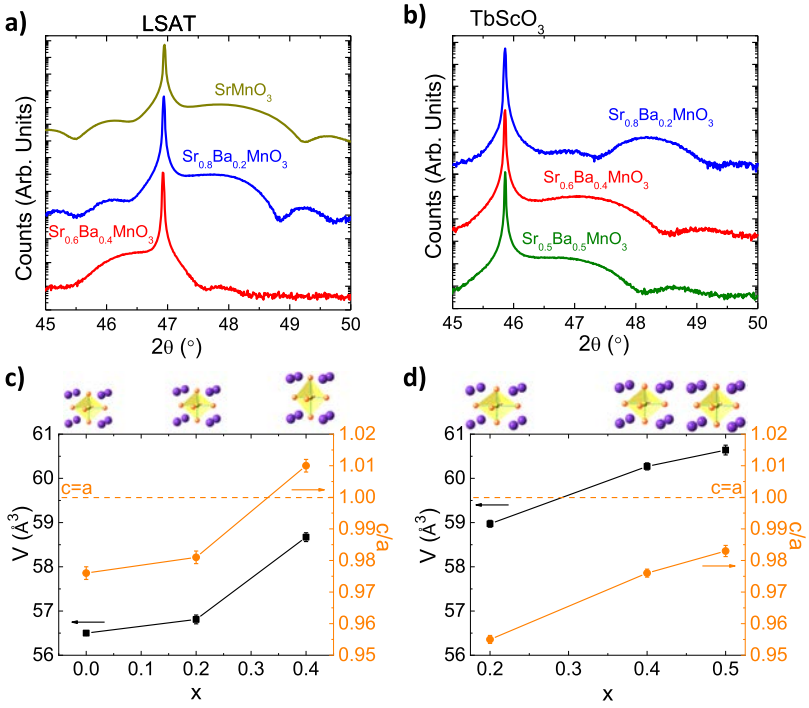

FIG. 1. θ/2θ XRD patterns around the symmetric 002 reflection for the SBMO films selected grown on (a) LSAT and (b) TSO substrates. Dependence of the cell volume (V) and tetragonality (c/a) on the Ba content (x) for samples grown on (c) LSAT and (d) TSO. A schematic representation of the strained unit cell is shown.

TABLE I. Values of the unit cell volume, tetragonality *c/a*, epitaxial strain, and T_{order} obtained in the $Sr_{1-x}Ba_xMnO_3$ perovskite thin films from XRD and wTF LE-μSR measurements.

Substrate	x	V (Å^3)	c/a	Strain (%)	T_{order} (K)
LSAT	0	56.50(4)	0.976(1)	1.63	171(4)
	0.2	56.81(2)	0.981(2)	1.24	159(1)
	0.4	58.65(1)	1.010(2)	−0.36	140(1)
TSO	0.2	58.97(1)	0.955(1)	3.39	187(5)
	0.4	60.42(1)	0.976(1)	1.82	118(3)
	0.5	60.75(2)	0.983(2)	0.94	124(4)

Low-energy muon spin spectroscopy (LE-μSR)[24,25] was used to determine T_{order} in all the previous films. This technique was successfully applied before in strained multiferroic SMO thin films.[14] T_{order} was determined from temperature scans in a weak transverse magnetic field (wTF) of B_{ext} = 10 mT applied perpendicular to the initial muon spin polarization and to the film surface. The data presented here were obtained with a muon implantation energy E_{imp} = 1 keV. This energy yields a mean implantation depth of the muon of about 5 nm and approximately 80% of the muons stopped in the SBMO films. In a wTF, the time evolution of the muon spin polarization is described by the relaxation function[26]

$$G_x(t) = f_T^{TF}\cos(\gamma_\mu B_l t + \phi)e^{-\lambda_T t} + f_L^{TF}e^{-\lambda_L t},$$

where $f_T{}^{TF}$ and $f_L{}^{TF}$ reflect the fraction of the muons having their spin initially transverse and longitudinal to the local magnetic field (B_l) direction, respectively, γ_μ is the gyromagnetic ratio of the muon, λ_T and λ_L are the relaxation rates, and ϕ is a phase offset. The fitting of the relaxation function $G_x(t)$ was performed using the *musrfit* program.[27] Above T_{order}, $f_T{}^{TF}$ is the full asymmetry since only B_{ext} is present inside the sample. Below T_{order}, the superposition of the small external B_{ext} and the internal AF magnetic fields leads to a strong dephasing of the signal, so $f_T{}^{TF}$ decreases to a level corresponding to the nonmagnetic fraction plus the background level. A decrease in $f_T{}^{TF}$ demonstrates static magnetism (see Ref. 14 for details).

Figures 2(a) and 2(b) display the transverse fraction $f_T{}^{TF}$ as a function of temperature in the 10 nm-thick SBMO films on LSAT and TSO, respectively. The data are normalized to the values in the paramagnetic regime at 300 K. The magnetic transition temperature is evidenced by the decrease in the transverse fraction $f_T{}^{TF}(T)/f_T{}^{TF}$ (300 K) at the ordering temperature. T_{order} is obtained by fitting the derivative curve of the data with a Gaussian curve and taking its center as T_{order}.[14] The corresponding values for T_{order} are listed in Table I. Interestingly, as clearly observed in Fig. 2, the magnetic transition is broader in the films with the largest strain levels (x = 0 on LSAT, and x = 0.2 on TSO), whereas it is sharper for the films with lower strain (x = 0.4 on LSAT; x = 0.5 on TSO). This broad decay has been previously observed in SMO films, and it was attributed to the existence of a distribution of ordering temperatures.[14] In order to ascertain whether there is a similar effect in the films studied here, we have used aberration-corrected scanning transmission electron microscopy (STEM). For these experiments, we have selected two samples grown on LSAT: (i) $SrMnO_3$ (SMO/LSAT) displaying a broad transition in $f_T{}^{TF}(T)$ and (ii) $Sr_{0.8}Ba_{0.2}MnO_3$ (SB20MO/LSAT) exhibiting a sharp transition in $f_T{}^{TF}(T)$. Figures 3(a) and 3(b) display the HAADF images (left panels) and geometrical phase analysis (GPA) relative deformation maps (right panels) of the SMO/LSAT and SB20MO/LSAT films viewed along the [110] zone axis, respectively. In both cases, the HAADF images show their very high crystal quality and the absence of structural defects within the film and at the interface with the substrate. The GPA in-plane relative deformation maps ($\varepsilon_{xx} = a_{film} - a_{subs}/a_{subs}$, where a_{film} and a_{subs} are the film and substrate in-plane lattice parameters, respectively) confirm that both films are fully strained, with no color variation between the substrate (reference lattice) and the film.

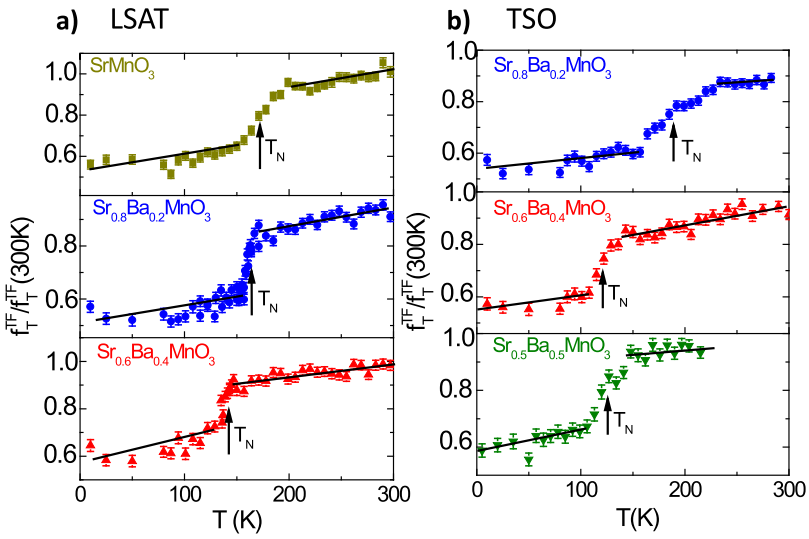

FIG. 2. Temperature dependence of the transverse fraction $f_T{}^{TF}$ of the muons normalized to the fraction at 300 K, determined from wTF LE-μSR measurements for 10-nm-thick $Sr_{1-x}Ba_xMnO_3$ films on (a) LSAT and (b) TSO. The arrows indicate the magnetic order temperature (see text).

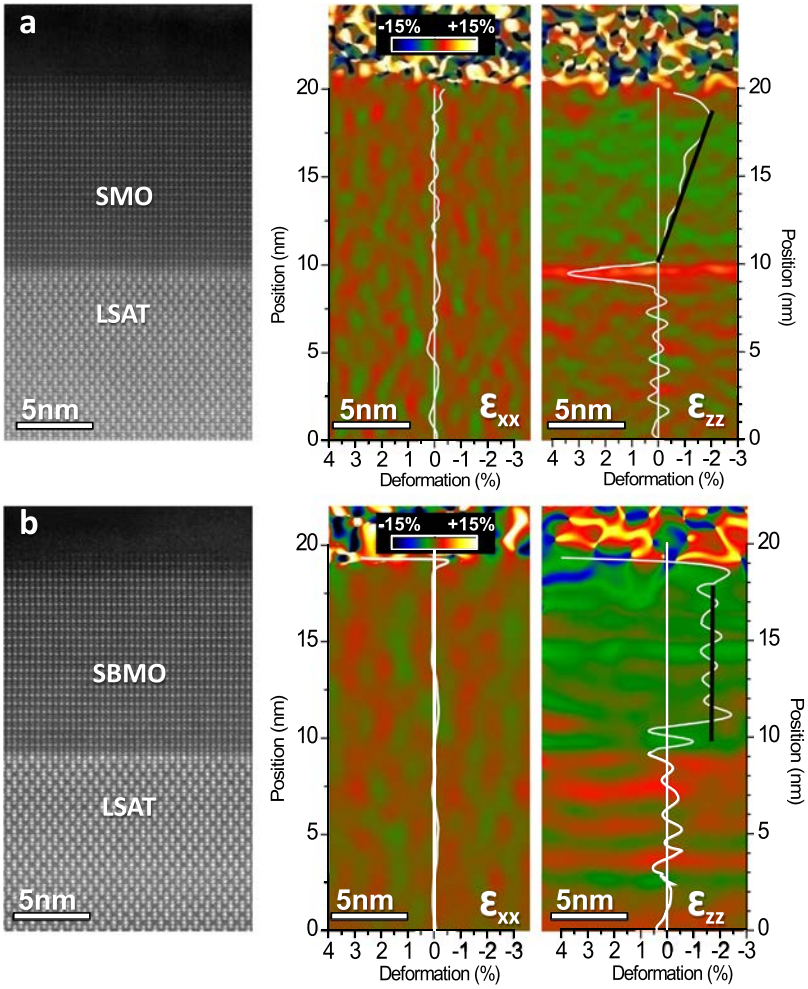

FIG. 3. STEM analysis of (a) SMO/LSAT and (b) SB20MO/LSAT films. Left panels: [110] cross-sectional HAADF-STEM images. Right panels: GPA in-plane (ε_{xx}) and out-of-plane (ε_{zz}) deformation maps. Map profiles are overlayered on the images. Black solid lines are guides for the eye.

The out-of-plane deformation maps, defined by the out-of-plane film (c_{film}) and substrate (c_{subs}) lattice parameters ($\varepsilon_{zz} = c_{film} - c_{subs}/c_{subs}$), unveil different strain states in both films: The SMO/LSAT film presents a compressive strain gradient (from $\varepsilon_{zz} \approx -0.5$ to $\varepsilon_{zz} \approx -2\%$), i. e., a gradual decrease in the *c*-parameter away from the interface (from $c_{film} = 0.3849$ nm to $c_{film} = 0.3807$ nm), whereas the SB20MO/LSAT film has a uniform deformation ($\varepsilon_{zz} \approx -1.6\%$). It is worth noting that the drop of the deformation values in the last unit cells near the surface in the films is due to damage caused by the sample preparation. Guzmán *et al.* demonstrated that this strain gradient is concomitant with a graded distribution of oxygen vacancies and additional out-of-plane polar distortions, which helps to accommodate the epitaxial strain at very low thickness. The additional off-centering of Mn cations, along the [001] axis, causes that the Mn-O-Mn bond-angle (α) departs from the 180° ranging from $\alpha \approx 178° \pm 3°$ close to the film-substrate interface to $\alpha \approx 172° \pm 3°$ at the film surface.[15] This gradient in α causes a variation of the superexchange paths that can yield local changes in T_N, which in turn gives rise to the broad magnetic transition observed in this sample. On the contrary, the SB20MO/LSAT film displays a uniform out-of-plane strain, and thus a constant Mn-O-Mn bond angle ($\alpha = 180°$) is observed within the experimental error.[15] This evidence explains the uniform magnetic transition temperature (i.e., the sharp transition) measured by LE-μSR in this sample.

The values of T_{order} in the SBMO films determined from wTF LE-μSR measurements as a function of the Ba content and the epitaxial strain induced by the LSAT and TSO substrates are shown in Figs. 4(a) and 4(b), respectively. Although a systematic theoretical study of the magnetic ordering as a function of the Ba content and strain is lacking, several first-principles calculations on the strain dependence of the magnetic ground state of SMO and $Sr_{0.5}Ba_{0.5}MnO_3$[6,8,9,22] have been performed. According to those studies, the predicted magnetic ground state at a low strain level (below 2%[6] or 3%[9] in SMO and below 3.5% in $Sr_{0.5}Ba_{0.5}MnO_3$[8]) is G-type AF for both compounds. The predictions for the SMO system were confirmed in our previous experimental work.[14] The SBMO films grown on LSAT are below that critical strain level (<3.5%), and so G-type AF order is expected. This assumption is confirmed by the experimental results: a monotonous decrease in T_N on increasing Ba doping is observed in the films grown on LSAT [Fig. 4(a)], which is a

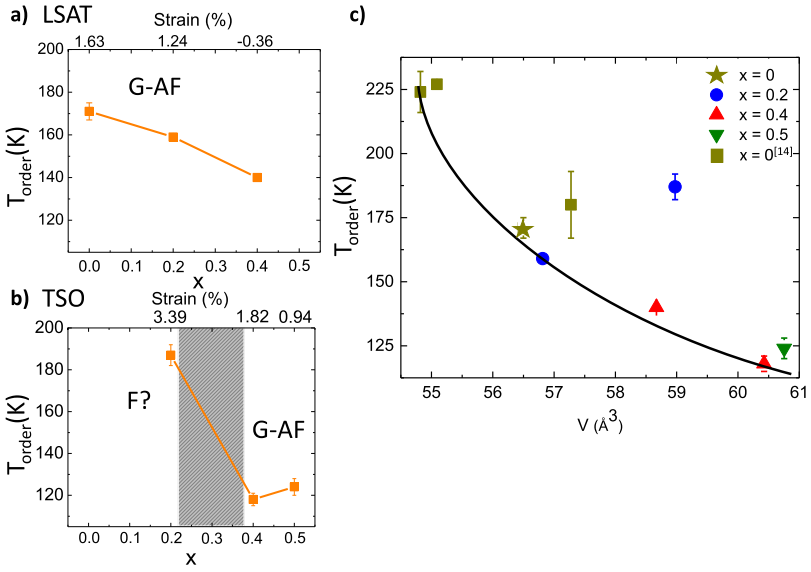

FIG. 4. Dependence of T_{order} on the Ba doping (x) and in-plane percent strain for the $Sr_{1-x}Ba_xMnO_3$ thin films deposited on (a) LSAT and (b) TSO. (c) Values of T_{order} as a function of the unit cell volume (V) for the studied films (see text for details). Green squares represent T_{order} of SMO (x = 0) bulk and thin films grown on $SrTiO_3$ and $LaAlO_3$ obtained by Maurel *et al.*[14] The solid line is a guide for the eye.

similar behavior to the one obtained in bulk samples[12,13,21] showing G-type AF magnetic order.

The SBMO films deposited on TSO [Fig. 4(b)] present a higher strain level than those on LSAT for the same Ba content. It is worth noting that the calculations mentioned before predict changes in the magnetic ground state depending on the tensile strain level. Thus, different AF orders for SMO (G-type, C-type, and A-type) have been predicted by increasing tensile strain.[6,9] Above a critical value of tensile strain (3.2%[6] or 4%[9]), a ferromagnetic (F) ground state is expected. This transition between AF (G-type) and F magnetic order driven by the strain was also predicted in $Sr_{0.5}Ba_{0.5}MnO_3$ and SMO.[8] The critical tensile strain needed to induce such an AF-F transition depends on the method used to perform the calculations: 5.2% and 3.5% for the *sPBEsol* and *PBE+U+J* methods for $Sr_{0.5}Ba_{0.5}MnO_3$, respectively, and 6.8%, 4.8%, and 3.2% for the *sPBEsol*, *PBE+U+J*, and *sPBE+Ueff* methods for SMO, respectively. Note that the critical strain values are lower as Ba content increases.[8] Moreover, Lee and Rabe showed that for all the AF orders, the value of T_N either decreases or remains constant by increasing the tensile strain, whereas the value of the ferromagnetic Curie temperature strongly increases by increasing the strain.[6] These predictions could explain the strong rise observed in T_{order} by increasing the strain (decreasing Ba content) in the SBMO films deposited on TSO substrates: from 118(3) K and 124(4) K for strain values of 1.82% and 0.94% (x = 0.4 and 0.5, respectively) to 187(5) K for 3.39% (x = 0.2). This behavior suggests a transition between an AF (G-type) order (low strain, high Ba content) to an F order (high strain, low Ba content). The experimental value of the tensile strain needed to induce such possible AF-F transition (≈3.3%) is in good agreement with the theoretical values determined by Lee and Rabe[6] and Chen and Millis[8] and a slightly lower than those predicted by Edström and Ederer.[9] Moreover, the theoretical models predict the coexistence of a ferroelectric/ferromagnetic ground state at high strain levels, increasing the interest of this compound. Unfortunately, the direct proof of this hypothesis using conventional magnetometric techniques was hindered by the huge paramagnetic signal arising from the substrate.

To unify the dependence of T_N on strain and Ba content in these films, we propose a model based on previous results on bulk materials.[21] According to the authors, T_N decreases on increasing the ionic radius of the A-site cation, which induces a change in the unit cell volume. It is noteworthy that in the present work, the unit cell volume is being modified by both Ba doping and epitaxial strain. The values of T_{order} determined from wTF-μSR measurements are plotted in Fig. 4(c) as a function of the room temperature unit-cell volume for the SBMO films deposited on TSO and LSAT substrates with Ba content ranging from x = 0 to x = 0.5. The values of T_N obtained by Maurel *et al.* for the x = 0 films grown on $SrTiO_3$ and $LaAlO_3$ are also displayed.[14] The figure shows a monotonic decrease in T_N as a function of the unit cell volume for those films with G-type AF order, regardless of the Ba content or the substrate used. Such behavior evidences a direct link between the two parameters in these AF films. On the other hand, the samples which do not follow such trend are the SMO films grown on $SrTiO_3$ (for which a C-type AF order was proposed[14]) and the x = 0.2 film on TSO. As mentioned above, our experimental results suggest that a plausible F order may occur in the SB20MO film deposited on TSO although an AF-type order different from G cannot be completely ruled out. All things considered, the unit cell volume, which determines the Mn-O-Mn distance, is the relevant parameter controlling T_N in SBMO thin films with G-type AF order. Taking into account that the unit cell volume can be modified by either epitaxial strain or the Ba content, the results shown in Fig. 4(c) indicate that both chemical strain and lattice strain are equivalent/exchangeable when determining the magnetic properties of the films with G-type AF order.

First-principle calculations have established a complex interplay between lattice strain, oxygen stoichiometry, and functional properties in $AMnO_3$ manganites, A being an alkaline-earth atom.[28] It is thus essential to rule out the possible influence of oxygen

vacancies or other extrinsic effects on the strain in our films. As explained before, an indirect analysis of the oxygen content carried out in SMO/LSAT films[15] revealed a gradient in the vacancies distribution, which originates a volume inhomogeneity of about ±0.8% with respect to the average value. This corresponds to a volume variation of ±0.4 Å^3, which is approximately accounted for by the error bar in the determination of T_N (see Table I). Therefore, the impact of cell volume change induced by moderate amount of oxygen vacancies on the Néel temperature is within the experimental error. Regarding the Ba doped films, X-ray absorption spectroscopy (XAS) measured in the SBMO sample that is most prone to have oxygen vacancies due to its large tensile strain and the low oxygen pressure during growth (i.e., 50% Ba-content film grown on the $GdScO_3$ substrate)[18] indicated the residual occurrence of Mn^{3+} within the experimental error. Thus, we can conclude that the majority presence of Mn^{4+} is a general feature in all our SBMO films.

Also, the distribution of the polar domains should be considered when analyzing the effect of strain on T_N in these films. A thorough study of their size and distribution was done in a 20-nm thick SMO/LSAT film. A combination of second harmonic generation (SHG) experiments and electrostatic force microscopy[10] showed the presence of micrometric-size polar domains, elongated along the cubic directions and markedly nonperiodical, which explains why we could not detect them by XRD. The polar axis lies in the film plane, equally probable along the ⟨110⟩ directions, as is also expected for the rest of the films analyzed in this work.[29] This was indeed confirmed by ABF-STEM direct imaging of cross sections of a $Sr_{0.7}Ba_{0.3}MnO_3$ film grown on TSO.[20] In spite of these observations, the epitaxial growth of the SBMO films on LSAT and TSO substrates is always cube-on-cube and is governed by the *A* cations of the ABO_3 perovskite structure (Sr/Ba in the films and La/Sr or Tb in the substrates), while the polar behavior arises from the shifts of Mn and O relative to that frame.[15,20] In conclusion, the existence of polar domains and domain walls has no influence in the determination of the epitaxial strain.

In summary, we have performed a systematic study of the dependence of the magnetic order temperatures in epitaxial SBMO thin films on the epitaxial strain and Ba content. From the experimental results, two main conclusions can be obtained: First, we reveal that the broadness of the magnetic transition occurring in the highly strained films is associated with a distribution of magnetic order temperatures within the film. This is due to the mechanism followed by these compounds to accommodate large epitaxial strain values, which yields a gradient in the out-of-plane lattice parameter along thickness and, therefore, a gradual change in the Mn–O–Mn bond angles. Second, we have found a clear correlation between T_N and the unit cell volume in the G-type AF films. This evidences that the Mn–O–Mn ionic distance, the gradual increase of which weakens the magnetic interaction, is the relevant parameter when it comes to determining the magnetic order temperature in SBMO films. Finally, from the comparison of the experimental results with different theoretical calculations performed until now, we suggest that a possible ferromagnetic order could emerge in the highly strained SB20MO film on TSO which could coexist with a ferroelectric order, making this material promising for both basic studies and technological applications.

This work has been supported by the Spanish Ministry of Science through Project Nos. MAT2017-82970-C2-1-R and MAT2017-82970-C2-2-R and by the Aragon Regional Government through Project Nos. E13_17R and E28_17R (*Construyendo Europa desde Aragón*). The LE-μSR measurements have been performed at the Swiss Muon Source SμS at the Paul Scherrer Institut, Villigen, Switzerland. The diffraction and microscopy studies have been conducted in the Laboratorio de Microscopías Avanzadas (LMA) at the Instituto de Nanociencia de Aragón (INA), Universidad de Zaragoza. The authors acknowledge the LMA-INA for offering access to their instruments and expertise.

REFERENCES

[1] N. A. Spaldin and M. Fiebig, Science **309**, 391 (2005).
[2] R. Ramesh and N. A. Spaldin, Nat. Mater. **6**, 21 (2007).
[3] S. W. Cheong and M. Mostovoy, Nat. Mater. **6**, 13 (2007).
[4] S. Bhattacharjee, E. Bousquet, and P. Ghosez, Phys. Rev. Lett. **102**, 117602 (2009).
[5] J. M. Rondinelli, A. S. Eidelson, and N. A. Spaldin, Phys. Rev. B **79**, 205119 (2009).
[6] J. H. Lee and K. M. Rabe, Phys. Rev. Lett. **104**, 207204 (2010).
[7] J. Hong, A. Stroppa, J. Íñiguez, S. Picozzi, and D. Vanderbilt, Phys. Rev. B **85**, 054417 (2012).
[8] H. Chen and A. J. Millis, Phys. Rev. B **94**, 165106 (2016).
[9] A. Edström and C. Ederer, Phys. Rev. Mater. **2**, 104409 (2018).
[10] C. Becher, L. Maurel, U. Aschauer, M. Lilienblum, C. Magén, D. Meier, E. Langenberg, M. Trassin, J. Blasco, I. P. Krug, P. A. Algarabel, N. A. Spaldin, J. A. Pardo, and M. Fiebig, Nat. Nanotechnol. **10**, 661 (2015).
[11] J. W. Guo, P. S. Wang, Y. Yuan, Q. He, J. L. Lu, T. Z. Chen, S. Z. Yang, Y. J. Wang, R. Erni, M. D. Rossell, V. Gopalan, H. J. Xiang, Y. Tokura, and P. Yu, Phys. Rev. B **97**, 235135 (2018).
[12] H. Sakai, J. Fujioka, T. Fukuda, D. Okuyama, D. Hashizume, F. Kagawa, H. Nakao, Y. Murakami, T. Arima, A. Q. R. Baron, Y. Taguchi, and Y. Tokura, Phys. Rev. Lett. **107**, 137601 (2011).
[13] H. Somaily, S. Kolesnik, J. Mais, D. Brown, K. Chapagain, B. Dabrowski, and O. Chmaissem, Phys. Rev. Mater. **2**, 054408 (2018).
[14] L. Maurel, N. Marcano, T. Prokscha, E. Langenberg, J. Blasco, R. Guzmán, A. Suter, C. Magén, L. Morellón, M. R. Ibarra, J. A. Pardo, and P. A. Algarabel, Phys. Rev. B **92**, 024419 (2015).
[15] R. Guzmán, L. Maurel, E. Langenberg, A. R. Lupini, P. A. Algarabel, J. A. Pardo, and C. Magén, Nano Lett. **16**, 2221 (2016).
[16] G. Giovannetti, S. Kumar, C. Ortix, M. Capone, and J. van den Brink, Phys. Rev. Lett. **109**, 107601 (2012).
[17] M. D. Glinchuk, E. A. Eliseev, Y. Gu, L.-Q. Chen, V. Gopalan, and A. N. Morozovska, Phys. Rev. B **89**, 014112 (2014).
[18] E. Langenberg, R. Guzmán, L. Maurel, L. Martínez de Baños, L. Morellón, M. R. Ibarra, J. Herrero-Martín, J. Blasco, C. Magén, P. A. Algarabel, and J. A. Pardo, ACS Appl. Mater. Interfaces **7**, 23967 (2015).
[19] V. Goian, E. Langenberg, N. Marcano, V. Bovtun, L. Maurel, M. Kempa, T. Prokscha, J. Kroupa, P. A. Algarabel, J. A. Pardo, and S. Kamba, Phys. Rev. B **95**, 075126 (2017).
[20] E. Langenberg, L. Maurel, N. Marcano, R. Guzmán, P. Štrichovanec, T. Prokscha, C. Magén, P. A. Algarabel, and J. A. Pardo, Adv. Mater. Interfaces **4**, 1601040 (2017).
[21] O. Chmaissem, B. Dabrowski, S. Kolesnik, J. Mais, D. E. Brown, R. Kruk, P. Prior, B. Pyles, and J. D. Jorgensen, Phys. Rev. B **64**, 134412 (2001).
[22] T. Barayaa, Y. Yang, H. J. Zhao, J. Íñiguez, and L. Bellaiche, Phys. Rev. Mater. **2**, 084404 (2018).

[23]R. D. Shannon and C. T. Prewitt, "Effective ionic radii in oxides and fluorides," Acta Crystallogr., Sect. B: Struct. Crystallogr. Cryst. Chem. **25**, 925 (1969).
[24]E. Morenzoni, T. Prokscha, A. Suter, H. Luetkens, and R. Khasanov, J. Phys.: Condens. Matter **16**, S4583 (2004).
[25]T. Prokscha, E. Morenzoni, K. Deiters, F. Foroughi, D. George, R. Kobler, A. Suter, and V. Vrankovic, Nucl. Instrum. Methods Phys. Res., Sect. A **595**(2), 317 (2008).
[26]E. Stilp, A. Suter, T. Prokscha, E. Morenzoni, H. Keller, B. M. Wojek, H. Luetkens, A. Gozar, G. Logvenov, and I. Božović, Phys. Rev. B **88**, 064419 (2013).
[27]A. Suter and B. M. Wojek, Phys. Procedia **30**, 69 (2012).
[28]A. Marthinsen, C. Faber, U. Aschauer, N. A. Spaldin, and S. M. Selbach, MRS Commun. **6**, 182 (2016).
[29]N. A. Pertsev, A. G. Zembilgotov, and A. K. Tagantsev, Phys. Rev. Lett. **80**, 1988 (1998).